ELSEVIER

Magnetic Resonance Imaging 21 (2003) 503–510

MAGNETIC RESONANCE IMAGING

Adaptive total linear least square method for quantification of mean transit time in brain perfusion MRI

XingFeng Li[a], Jie Tian[a,*], EnZhong Li[a,b], XiaoXiang Wang[a], JianPing Dai[b], Lin Ai[b]

[a]*Medical Image Processing Group, Institute of Automation, Chinese Academy of Sciences, Beijing, China*
[b]*Department of Radiology, Tian Tan Hospital, Beijing, China*

Received 27 September 2002; accepted 24 January 2003

Abstract

Absolute quantification of cerebral blood flow (CBF), cerebral blood volume (CBV), and mean transit time (MTT) are of great relevance for clinical applications. One of the widely used methods for quantification of these parameters is γ-variate fitting. Traditional nonlinear regression methods for γ-variate fitting are inaccurate and computationally demanding. In this study, we developed an adaptive total least square method (ATSSL) to fit a γ-variate function to the delayed concentration-time course. For each concentration-time curve, the beginning and ending time point of the curve are adaptively determined online. After the curves were fitted, a robust method for automatically determination of arterial input function (AIF) from whole and region of interest (ROI) was developed. Using the obtained AIF and fitted γ-variate concentration-time curve, the MTT, CBV, and CBF were calculated by utilizing singular value decomposition algorithm. Computer simulations show that the suggested method is adaptive, reliable, and insensitive to noise. Comparison with the traditional nonlinear regression method indicated that the presented method is more accurate and faster to determine the CBV, CBF and MTT.

Keywords: Arterial input function; Mean transit time; Adaptive total linear least square; Concentration-time curves; Blood flow

1. Introduction

There are two widely used methods for absolute quantification of the mean transit time (MTT), cerebral blood volume (CBV), and cerebral blood flow (CBF) with dynamic susceptibility contrast-enhanced MRI (DSC-MRI) [1]. One of these is the tissue impulse response method and the other is the γ-variate fitting method. The former method uses the calculated tissue-residue function which is calculated by singular value decomposition (SVD) [2–4]. Based on the residue function and its derivative, the CBF, CBV, and MTT can be calculated. The latter utilizes the γ-variate fitting technique to eliminate recirculation, and the CBF, CBV, and MTT are calculated according to the fitted concentration-time curves [5–8]. Most of these methods adopted the nonlinear regression algorithm such as Levenberg-Marquart (LM) for curve fitting. The major drawback of the method is inaccurate and computationally demanding especially the free parameters are many. Another drawback of the LM fitting method is that it requires carefully chosen initial values to guarantee the success fitting [8]. When taking into account the delay between arterial and tissue response in the γ-variate function fitting, this method generally did not produce satisfactory results [2]. Moreover, due to numerical computation, this algorithm may introduce numerical noise [1].

The purpose of the present study was to develop a method for improving the γ-variate fitting method for obtaining more accuracy absolute quantification of the MTT, CBV, and CBF. By considering the trace delay [4], an adaptive total least square method for γ-variate fitting was proposed. Then we introduced the robust and accurate method for determination of arterial input function (AIF). Finally, absolute quantification of the MTT, CBV, and CBF

Grant sponsors: National Science Fund for Distinguished Young Scholars of China; Special Project of National Grand Fundamental Research 973 Program of China; National Natural Science Foundation Grant of China; National High Technology Development Program of China (863 Program).

Grant numbers: 60225008, 2002CCA03900, 30270403, 69931010, 60172057, 60071002, 60072007; 2002AA234051.

* Corresponding author. Tel.: +86-10-62532105; fax: +86-10-62527995.

E-mail address: tian@doctor.com (J. Tian)

0730-725X/03/$ – see front matter
doi:10.1016/S0730-725X(03)00075-4

were calculated by means of SVD method. We also report our comparison results with the nonlinear regression method for determination absolute quantification of these parameters.

2. Methods

2.1. Indicator dilution theory

The relation between concentration and signal intensity is as follows [9]:

$$C_m(t) = -k \cdot \ln \frac{S(t)}{S(t_0)} \tag{1}$$

where $C_m(t)$ is the measured concentration of gadolinium diethylene triamine pentaacetic acid (Gd-DTPA) with respect to time, k is a proportionality constant that is inversely proportional to the TE and depends on the MR scanner (for simplicity, a value of 1 for k is assumed throughout the rest of the study), $S(t)$ is the MRI signal intensity with respect to time, and $S(t_0)$ is the baseline MRI signal before the presence of Gd-DTPA and after steady-state magnetization has been achieved. To acquire $S(t_0)$, one step M-estimator (see appendix) was chosen to filter the first 2-6 image before the trace appear from the brain perfusion image sequence.

MTT can be calculated by using the following equations [5,6,10,11]:

$$MTT = \frac{\int C(t)dt}{C_{\max}} = \frac{CBV}{CBF} \tag{2}$$

where $C_{\max}$ is the maximum of the $C(t)$, $C(t)$ is the idealized bolus which is given by:

$$C(t) = C_m(t) \otimes^{-1} AIF(t),\ t_o \le t \tag{3}$$

where t_0 is the appear time of the tissue; $\otimes^{-1}$ represents the deconvolution operation, $AIF(t)$ is the measured AIF.

After $C_m(t)$ was determined, the CBV can be calculated using the relation:

$$CBV = \frac{k_H}{\rho} \cdot \frac{\int C_m(t)dt}{\int AIF(t)dt} \tag{4}$$

where $k_H = 0.73$; $\rho = 1.04$ *g/ml*.

Finally, the CBF can be calculated as:

$$CBF = \frac{CBV}{MTT} \tag{5}$$

2.2. Data acquisition

Patients data were acquired using a 3-T GE Signa scanner (GE Medical Systems, Milwaukee, WI, USA) with 5 mm slice thickness, 1 mm interslice gap, 24×24 cm^2 field of view (FOV) and 14 slices per volume. A single-shot gradient-echo EPI sequence (TR/TE = 2000 msec/30 msec) was used to perform the bolus tracking, with the sequence started at the same time after the Gd-DTPA injection (0.1/mmol/kg). The bolus was injected at a rate of 5 mL/sec, using an MR-compatible power injector (Medrad Inc., Pittsburgh, PA, USA). The study was approved by local ethics committee and consented by the patients.

2.3. Determination of delay and first pass ending time

We developed a method to adaptive determine the time widow (the appear time and first pass ending time) of the concentration-time curve. Because the blood flow velocity is different in different tissue, the appear time t_0 in Eq. (2) and the first pass ending time t_e is different. An adaptive method was developed to determine the tissue appear time t_0 and t_e. In the first step, for each concentration-time curve, we search for the time $t_{\max}$ when tissue concentration reaches its maximum. We set t_0, if at that point it fulfilled the following conditions:

if

$$\begin{aligned}(C_m(t_{i+1}) - C_m(t_i) > 0)\ \&\ (C_m(t_{i+2}) - C_m(t_{i+1}) \\ > 0)\ \&\ (C_m(t_{i+3}) - C_m(t_{i+2}) \\ > 0)\ \&\ (t_{i+3} < t_{\max})\end{aligned} \tag{6}$$

where $i > 1$

and if

$$\frac{C_m(t_{i+1}) - C_m(t_i)}{C_m(t_i)} \ge 1 \tag{7}$$

then

$$t_0 = t_i$$

else

$$t_0 = t_i + 1$$

In the same way, the end time t_e can be determined if it fulfilled the follow conditions:

if

$$\begin{aligned}(C_m(t_i) - C_m(t_{i+1}) < 0)\ \&\ (C_m(t_{i-1}) - C_m(t_{i-2}) \\ < 0)\ \&\ (C_m(t_{i-2}) - C_m(t_{i-3}) \\ < 0)\ \&\ (t_i > t_{\max})\end{aligned} \tag{8}$$

where $i > 1$

and if

$$\frac{C_m(t_{i-1}) - C_m(t_i)}{C_m(t_i)} \ge 1 \tag{9}$$

then

$$t_e = t_i$$

else

$$t_e = t_i - 1$$

2.4. Data analysis (total linear square for curve fitting)

To denoise and eliminate tracer recirculation, $C_m(t)$ curves were fitted to the gamma function [12,13]:

$$C_m(t) = K(t - t_0)^{\alpha} e^{-\frac{t-t_0}{\beta}}, \; t > t_0 \tag{10}$$

where t is the time after injection, K is constant scale factors, α, β are γ-variate parameters.

When fitting nonlinear Eq. (10), many numerical methods such as Gauss-Newton method, steepest descent method, and LM method (see [14] and references therein) can be used. For nonlinear function fitting, the initial values are important to convergence and efficiency for curve fitting. Thus, using a more complex nonlinear model does not always improve parameter accuracy, because the data are too noisy or the number of measurements is too low. In contrast, enhancing the data by SVD based methods before parameters estimation and exploiting prior knowledge as much as possible, clearly helps to improve the accuracy. In linear regression such as moment estimator method [12], weighted least square method [13] can be adopted for this purpose. However, these methods trend to be inaccurate, because the appearance time t_0 is experiential determined. In this study, we present an adaptive minimum-norm total linear least square (AMN-TLLS) [15-17] method for $C_m(t)$ fitting.

Logarithm Eq. (10) [13], we get:

$$\ln(C_m(t)) = \ln(K) + \alpha \ln(t - t_0) - \frac{1}{\beta}(t - t_0), \; t > t_0 \tag{11}$$

or

$$y_i = b_0 + b_1 x_{i1} + b_2 x_{i2} \tag{12}$$

where $y_i = \ln(C_m(t_i))$, $b_0 = \ln(K)$, $b_1 = \alpha$, $b_2 = -\frac{1}{\beta}$, $x_{i1} = \ln(t_i - t_0)$, $x_{i2} = t_i - t_0$.
Eq. (12) can be written as:

$$\begin{aligned} y_1 &= b_0 + b_1 x_{11} + b_2 x_{12} \\ y_2 &= b_0 + b_1 x_{21} + b_2 x_{22} \\ &\cdots \quad \cdots \quad \cdots \quad \cdots \\ y_i &= b_0 + b_1 x_{i1} + b_2 x_{i2} \end{aligned}$$

or

$$\begin{bmatrix} y_1 \\ y_2 \\ \cdots \\ y_i \end{bmatrix} = \begin{bmatrix} 1 & x_{11} & x_{12} \\ 1 & x_{21} & x_{22} \\ \cdots & \cdots & \cdots \\ 1 & x_{i1} & x_{i2} \end{bmatrix} \cdot \begin{bmatrix} b_0 \\ b_1 \\ b_2 \end{bmatrix}$$

In the following, we shall use the short-hand matrix notion

$$Y = X \cdot B \tag{13}$$

where

$$Y = \begin{bmatrix} y_1 \\ y_2 \\ \cdots \\ y_i \end{bmatrix}, \quad X = \begin{bmatrix} 1 & x_{11} & x_{12} \\ 1 & x_{21} & x_{22} \\ \cdots & \cdots & \cdots \\ 1 & x_{i1} & x_{i2} \end{bmatrix}, \quad B = \begin{bmatrix} b_0 \\ b_1 \\ b_2 \end{bmatrix}.$$

Solving Eq. (13) need to minimize

$$|X \cdot B - Y|$$

where $|\,|$ denotes the vector norm.

From Eq. (13) we have

$$B = X^{+} \cdot Y \tag{14}$$

where X^{+} is the Moore Penrose inverse of X. To solve Eq. (14), the most robust method SVD is adopted [2,15–17].

By using SVD, matrix X^{+} in Eq. (14) can be decomposed as

$$X^{+} = V \cdot W \cdot U^{T} \tag{15}$$

where W is a diagonal matrix, V and U^T are orthogonal and transpose orthogonal matrices, respectively. Given this pseudo inverse, X can be expressed as

$$B = V \cdot W \cdot U^{T} \cdot Y \tag{16}$$

From Eqs. (13) and (16), we have $K = e^{b_0}$, $\alpha = b_1$ *and* $\beta = -\frac{1}{b_2}$.

2.5. Determination of the AIF

To achieve reliable and accurate AIF despite the existence of noise, we developed a program to allow selection of pixels located in brain major arteries. The method can be divided into three steps. In the first step, parameters of fitted tissue concentration-time curve such as the full width at half maximum (FWHM), the maximum concentration (MC), and the moment of maximum concentrations (MMC) were calculated pixel by pixel from the whole brain or ROI. The pixels were selected to satisfy both of the following conditions:

$$FWHM_{AIF} < Sort(FWHM)_{(c)} \tag{17}$$

$$MMC_{AIF} < Sort(MMC)_{(c)} \tag{18}$$

where *Sort* is the sort operation of the sequence, $\mathrm{FWHM_{AIF}}$ is the FWHM of the AIF, $\mathrm{MMC_{AIF}}$ is the MMC of the AIF. $Sort(FWHM)_{(c)}$ is the c smallest of the sorted FWHM; $Sort(MMC)_{(c)}$ is the c smallest of the sorted MMC.

In the second step, only these pixels of the preselected

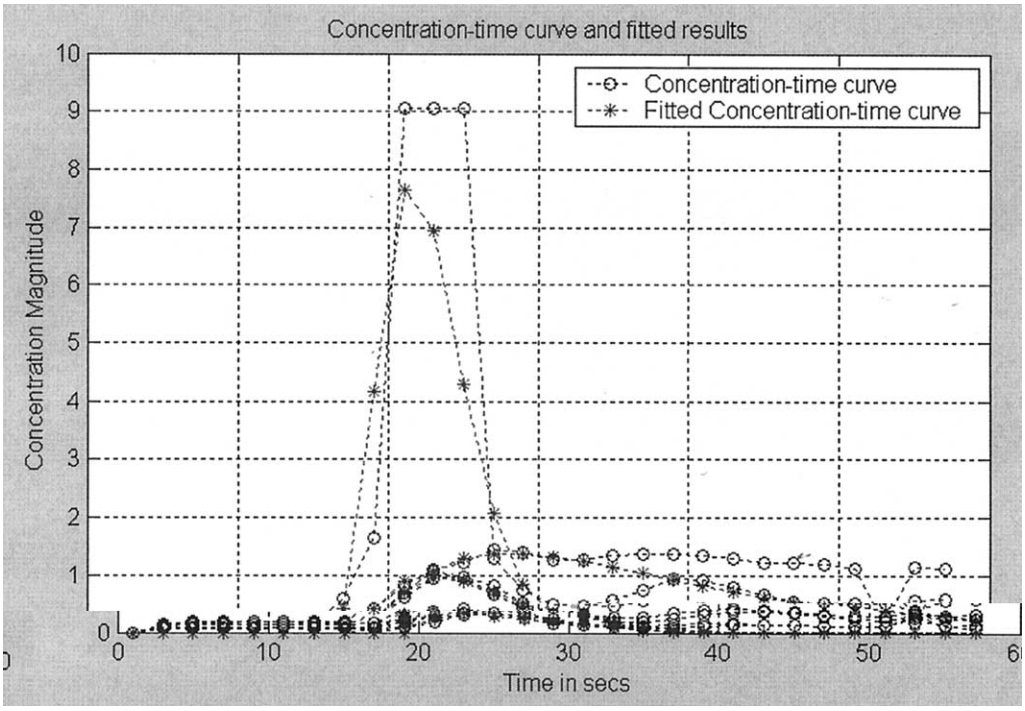

Fig. 1. Concentration-time curve and its fitted results by using ATLLS method.

pixels were considered to have a maximum concentration of at least 75% of the highest value. In the third step, one step M-estimator [18] was used to denoise (see appendix).

To calculate the decomvolution in Eq. (2), SVD method was used. We deconvolved the tissues concentration-time curve with AIF over the whole range of dynamical images [1].

Eq. (3) can be express as:

$$C_m(t_k) = \sum_{k=0}^{i} AIF(k) \cdot C(t_k - k) \tag{19}$$

or matrix form:

$$\begin{bmatrix} C_m(t_0) \\ C_m(t_1) \\ \cdots \\ C_m(t_i) \end{bmatrix} = \begin{bmatrix} \mathrm{AIF}(t_0) & 0 & \cdots & 0 \\ \mathrm{AIF}(t_1) & \mathrm{AIF}(t_0) & \cdots & 0 \\ \cdots & \cdots & \cdots & 0 \\ \mathrm{AIF}(t_i) & \mathrm{AIF}(t_i-1) & \cdots & \mathrm{AIF}(t_0) \end{bmatrix} \cdot \begin{bmatrix} \mathrm{C}(t_0) \\ \mathrm{C}(t_1) \\ \cdots \\ \mathrm{C}(t_i) \end{bmatrix} \tag{20}$$

C(t) can be obtained for the Eq. (20) by truncated SVD method [2]. Absolute value of the MTT was determined from Eq. (2).

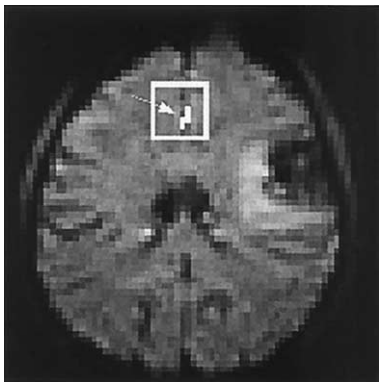

Fig. 2. An example of the extraction of anterior cerebral artery used ATLLS fitting method. The white rectangular line shows the mask ROI drawn around the anterior cerebral artery.

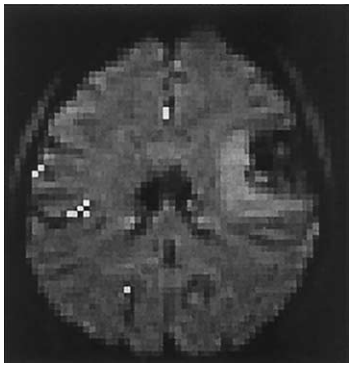

Fig. 3. By utilizing the ATLLS method, the possible artery location in the brain was determined. The white pixels represented the location of arteries, including possible noise pixels.

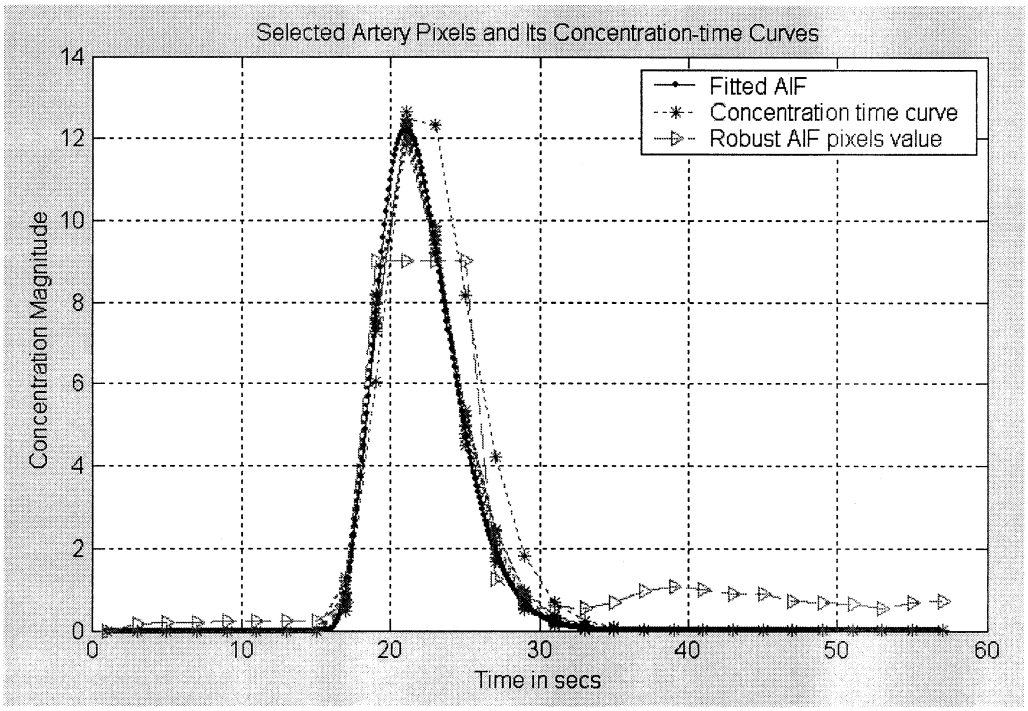

Fig. 4. Curve fitting results by using ATLLS method. The parameters of AIF were determined to be: $K = 0.073$, $\alpha = 6.263$, $\beta = 0.984$, $t_a = 15$ sec, $t_e = 31$ sec. The t_a and t_e of AIF were determined by using one step M-estimator.

3. Results

Simulations were performed by utilizing commercial software package (MATLAB, Mathworks, Natick, MA, USA). In the simulation, we used the first 2-6 images (before the apparent of bolus) and developed the robust method to allow accurate estimate the baseline signal $S(t_0)$.

Figs. 1–7 show the simulation results. Fig. 1 shows the concentration-time curves fitted results. We used the uniform random sample method to select the position of the concentration. The number of the curve is 6. It can be seen that ATLLS method fits all the random sample curves. The appear time of tissue concentration-time curves t_0 were traced by the suggested ATLLS method, as shown in Fig. 1.

In Figs. 2 and 3, the white pixels stand for the selected possible artery pixels by computer program. We drew a 10 $\times$ 10 masking in the artery region and set coefficient c = 50 in Eqs. (17,18). Fig. 2 shows an artery region (shown by arrow) extracted using our method, together with the mask ROI shown by a white rectangular line. Adjusting coefficient c = 500 in Eqs. (17) and (18), the artery pixels (white pixels) in the whole image region search results are shown in Fig. 3.

Fig. 4 shows the AIF and its fitted results. We fitted all curves by using ATLLS. The AIF was fitted after the artery pixels had been smoothed by robust filter.

As reported previously [19], the quality of the fit depends on the signal noise rate (SNR) of the raw data. Because of noise and tracer dispersion, there were some curves still can not be fitted. Eliminating these pixels, the CBF, CBV, and MTT map can be calculated. The results are shown in Figs.

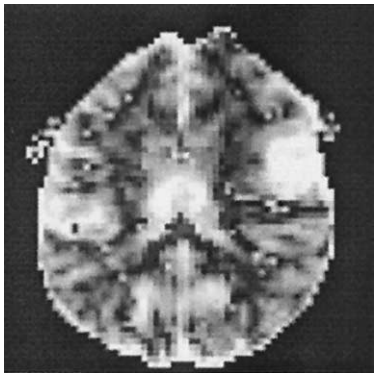

Fig. 5. An example of CBV map generated by using Eq. (4).

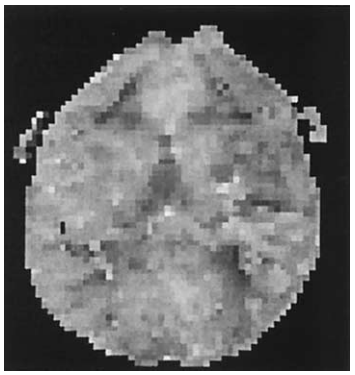

Fig. 6. An example of MTT map obtained by using Eq. (2).

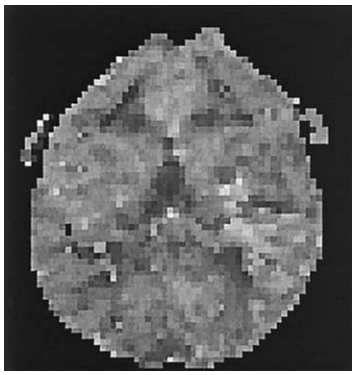

Fig. 7. An example of CBF map produced by using Eq. (5).

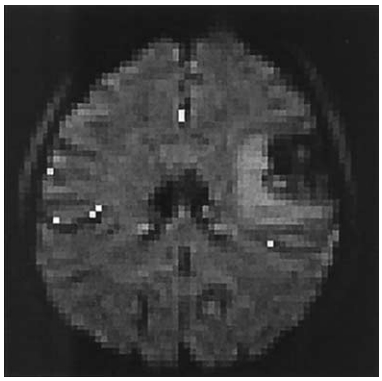

Fig. 9. LM method for the artery pixels searching, artery pixels were chosen according to Rempp et al.'s method [5], the coefficient before the standard deviation was set to be 0.7.

5-7. By virtue of this algorithm, more than 2344 of 2441 (image region) curves had been fitted by using ATLLS algorithm.

4. Discussion

4.1. Comparison ATLLS with the current nonlinear regression

To compare the ATLLS method with LM method for absolute quantification, we used the LM algorithm to calculate the CBV, CBF, and MTT.

Figs. 8–10 show the results produced by LM method. The initial values of Eq. (10) for K, α, β, and t_0 were set to be 2, 5, 1, and 13, and the ending point was set to 31 secs. Because the existence of noise, there were some curves can not be fitted by this method, we break the loop when the iterations over 100 times.

We used the same random sample method as ATLLS to select the position of the concentration time curves for γ-variate fitting. Compare Fig. 8 with Fig. 1, it is clear that LM method is more often inaccurate for estimating tissue concentration-time curve. It can also be seen that the appear time are not fitted the true concentration-time curves.

In Fig. 9, the artery pixels were selected by using LM algorithm and Rempp et al.'s method. The white pixels represent the selected artery in the whole brain. Using these pixels, the AIF was fitted by LM method, as shown in Fig. 10.

The CBV, CBF, and MTT maps obtained by LM method

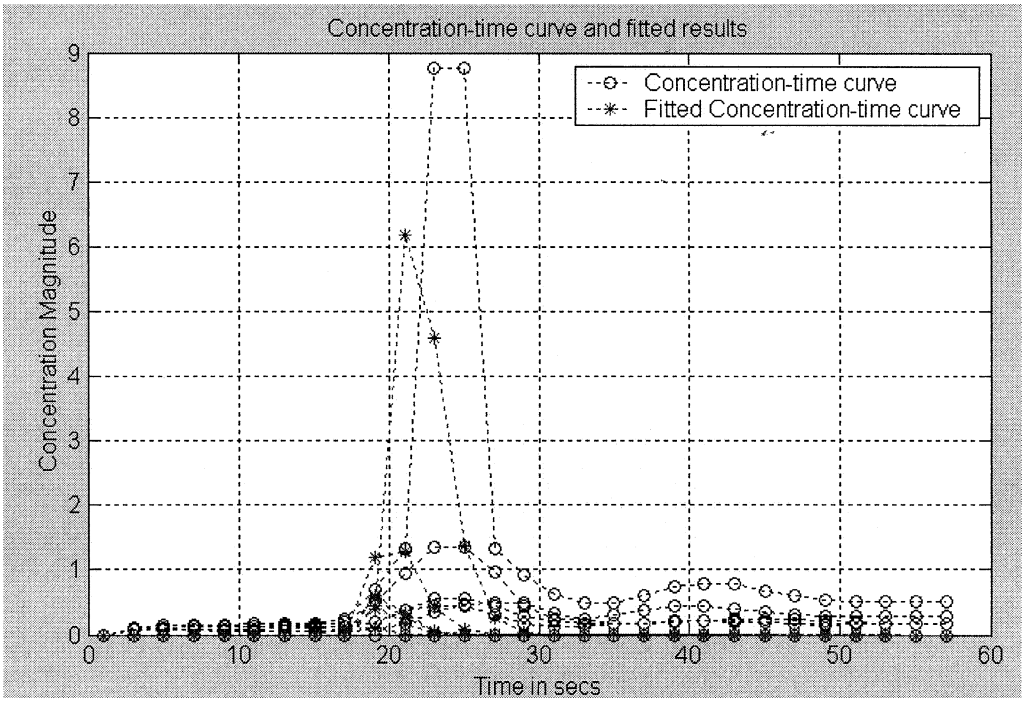

Fig. 8. Concentration-time curve and its fitted results by using LM method.

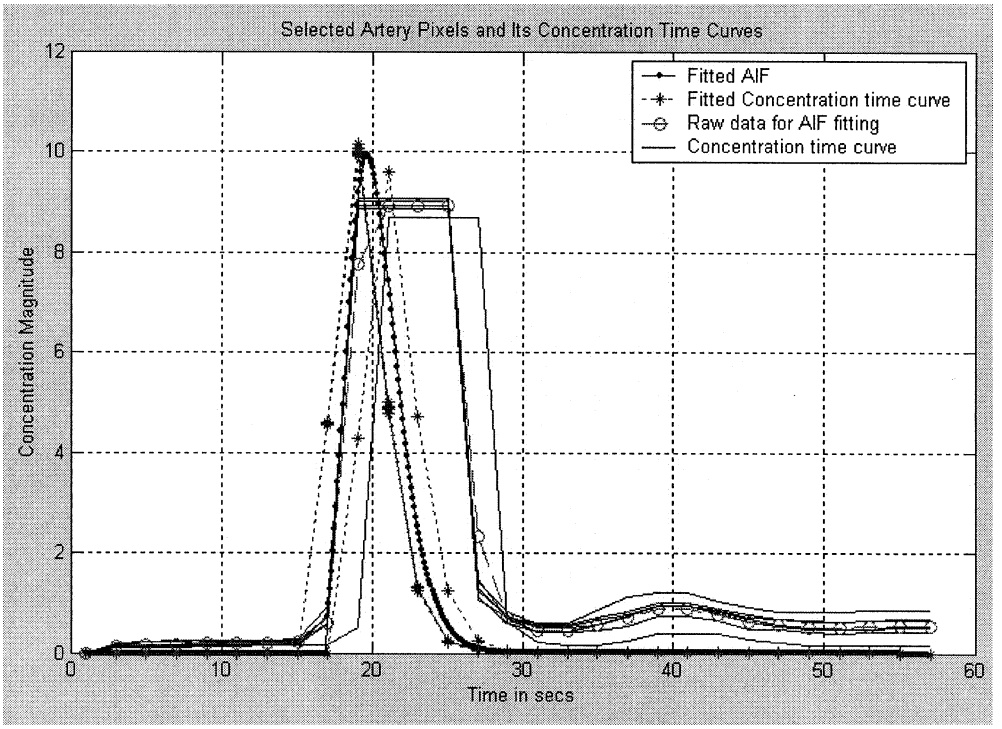

Fig. 10. Fitting results of AIF curve by using LM method, the parameters of γ-variate were: $K = 2.013$, $\alpha = 5.140$, $\beta = 0.721$, and $t_0 = 17$ secs. The t_0 of AIF were determined by using one step M-estimator, and because of temporal resolution limitation, we omitted the decimal parts.

are similar to the ATLLS method by visual; due to space limit, we do not show the figures here.

4.2. Comparison different methods for determined AIF

Many methods for determined AIF were proposed Rempp et al. [5] reported an interactive computer program to determine AIF automatically. This method is fast, accurate, objective, but sensitive to noise. Similar method was developed by Mark Rijpkema et al. [20]. A new interactive program was suggested by Smith et al. [6] for determining the AIF. This method is robust to noise but subjective and time consuming for picking out noise pixels by manual. To acquire high robust to noise, Murase et al. [21] presented the fuzzy clustering method for determining AIF. In using this method, a mask ROI was first drawn around the targeted artery. Then FCM cluster was used to segment the artery pixels in the mask ROI. The AIF was obtained from the mean concentration-time curve in those regions. The method is complex and difficult to choose the optimal parameters of the cluster. Moreover, the fuzzy rules of the cluster are subjective and also difficult to determine.

To determine the AIF, we developed method based on order statistics. We do not calculate the standard deviation as done by Rempp. The only thing need to do is determination the order number. This can be done by several tries. Rempp et al.'s method for selected AIF pixels needs to adjust the coefficient before the preselected pixels. In most case, this parameter required to be adjusted.

To deconvolve with tissue concentration-time curve, we capitalized on SVD algorithm to perform deconvolution and thus more robust to the numerical inaccuracy [17]. The other advantage is the uniform of the algorithm. When idealized bolus was calculated, we used the SVD algorithm to deconvolve tissue concentration-curve time with AIF. When we fitted the AIF and tissue time concentration curve by using ATLLS, the same SVD algorithm can be used again.

We investigated the feasibility of using ATLLS method to accuracy fit the delayed tissue concentration time curves, and therefore more accurate to determine absolute quantification of the perfusion parameters. Moreover, we proposed a new method for determining AIF from both ROI and whole image. The advantage of the method is accurate, objective, and robust to noise. Further study is needed to prove the clinical value of this technique.

5. Conclusions

Taking into account the delay of tissue concentration-time curve, we presented ATLLS method for accuracy determination of the absolute quantification of perfusion parameters. The method first estimates the appear time and first pass ending time, then using SVD method for γ-variate fitting.

Furthermore, this study presented a robust method to determine the AIF in cerebral perfusion imaging. The

method based on robust statistical theory allows for more accurate and robust extraction of the arterial pixels and determination AIF curve.

In short, it possible to more accurate determines the absolute CBV, CBF, and MTT by using ATLLS method.

Acknowledgments

We thank medical image processing group of institute of automation, Chinese Academy of Sciences, for their valuable comments. He HuiGuang, PhD, Chen Hong, MSc, and Wang XiaoXiang, MSc are also gratefully acknowledged for their valuable programming discussions.

Appendix

This appendix demonstrates the principle of one step M-estimator [18]. For simply, we take the estimation of $S_0(t)$ for example.

$$S_0(t) = \frac{1.28(MADN)(MU - L) + MB}{n - L - MB}$$

$$MADN = \frac{MAD}{0.6745}$$

MAD is the median absolute deviation statistic, calculated as follows:

$$MAD = median(|S_{02}(t) - M|, |S_{03}(t) - M|, \cdots, |S_{06}(t) - M|)$$

where

M = $median(S_{02}(t), S_{03}(t), \cdots, S_{06}(t))$ is the sample median;

$S_{02}(t), S_{03}(t) \cdots S_{06}(t)$ are the baseline image before the appears of trace;

MU is the number of outliers greater than the median;

L is the number of outliers smaller than the median;

MB is the sum value that for not labeled outliers.

For two dimensions, the estimator was set to 3×3, the principle of which is similar.

References

[1] Perkio J, Aronen HJ, Kangasmaki A, Liu Y, Karomen J, Savolainen S, Østergaard L. Evaluation of four postprocessing methods for determination of cerebral blood volume and mean transit time by dynamic susceptibility contrast imaging. Magn Reson Med 2002;47:973–81.

[2] Østergaard L, Weisskoff RM, Chesler DA, Gyldensted C, Rosen BR. High resolution measurement of cerebral blood flood flow using intravascular tracer bolus passages. Part I: Mathematical approach and statistical analysis. Magn Reson Med 1996;36:715–25.

[3] Østergaard L, Sorensen AG, Kwong KK, Weisskoff RM, Gyldensted C, Rosen BR. High resolution measurement of cerebral blood flood flow using intravascular tracer bolus passages. Part II: Experimental comparison and preliminary results. Magn Reson Med 1996;36:726–36.

[4] Calamante F, Gadian DG, Connelly A. Delay and dispersion effects in dynamic susceptibility contrast MRI: simulations using singular value decomposition. Magn Reson Med 2000;44:466–73.

[5] Rempp KA, Brix G, Wenz F, Becker CR, Friedemann, Lorenz WJ. Quantification of regional cerebral blood flow and volume with dynamic susceptibility contrast-enhanced MR imaging. Radiology 1994;193:637-41.

[6] Smith AM, Grandin CB, Duprez T, Mataigne F, Cosnard G. Whole brain quantitative CBF, CBV, and MTT measurements using MRI bolus tracking: implementation and application to data acquired from hyperacute stroke patients. J Magn Reson Imag 2000;12:400–10.

[7] Makiranta MJ, Lehtinen S, Jauhiainen JPT, Oikarinen JT, Pyhtinen J, Teronenl O. MR perfusion, diffusion and BOLD imaging of methotrexate-exposed swine brain. J Magn Reson Imag 2002;15:511–9.

[8] Benner T, Heiland S, Erb G, Forsting M, Sartor K. Accuracy of γ-variate fits to concentration-time curves from dynamic susceptibility-contrast enhanced MRI: influence of time resolution, maximal signal drop and signal-to-noise. Magn Reson Imag 1997;15:307–17.

[9] Rosen BR, Belliveau JW, Vevea JM, Brady TJ. Perfusion imaging with contrast agents. Magn Reson Med 1990;14:249–65.

[10] Meier P, Zierler KL. On the theory of the indictor-dilution method for measurement of blood flow and volume. J Appl Physiol 1954;6:731–44.

[11] Zierier BKL. Theoretical basis of indicator-dilution methods for measuring flow and volume. Cirs Res 1962;10:393–407.

[12] Thompon HK, Starmer CF, Whoalen RE, McIntosh HD. Indicator transit time considered as a gamma variate. Circ Res 1964;14:502–15.

[13] Starmer CF, Clark DO. Computer computations of cardiac output using the gamma function. J Appl Physiol 1970;28:219–20.

[14] Rawlings JO, Pantula SG, Dickey DA. Applied regression analysis: a research tool. New York: Springer, 1998. p. 485–514.

[15] Van Huffel S. Recent advances in total least squares techniques and errors-in-variables modeling. SIAM Philadelphia, Proceedings of the second international workshop on total least squares and errors-in-variables modeling, 1997. p. 307-18.

[16] Van Huffel S, Vandewalle J, De Roe MCh, Willems JL. Reliable and efficient deconvolution technique based on total linear least squares for calculating the renal retention function. Med Biol Eng Comput 1987;25:26–33.

[17] Press WH, Teukolsky SA, Vetterling WT, Flannery BP. Numerical recipes in C: the art of scientific computing. 2nd ed. Oxford: Cambridge University Press, 1993.

[18] Wilcox R. Fundamentals of modern statistical methods: substantially improving power and accuracy. New York: Springer Press, 2001. p. 139–58.

[19] Boxerman JL, Rsen BR, Weisskoff RM. Signal-to-noise analysis of cerebral blood volume maps from dynamic NMR imaging studies. J Magn Reson Imag 1997;7:528–37.

[20] Pijpkema M, Kaanders JHAM, Joosten FBM, van der Kogel AJ, Heerschap A. Method for quantitative mapping of dynamic MRI contrast agent uptake in human tumors. J Magn Reson Imag 2001;14:457–63.

[21] Murase K, Kikuchi K, Miki H, Shimizu T, Ikezoe J. Determination of arterial input function using fuzzy clustering for quantification of cerebral blood flow with dynamic susceptibility contrast-enhanced MR imaging. J Magn Reson Imag 2001;13:797–806.